Journal of Materials Science: Materials in Medicine (2018) 29:89
https://doi.org/10.1007/s10856-018-6100-2

TISSUE ENGINEERING CONSTRUCTS AND CELL SUBSTRATES

Original Research

Dynamics of tissue ingrowth in SIKVAV-modified highly superporous PHEMA scaffolds with oriented pores after bridging a spinal cord transection

Aleš Hejčl[1,2] · Jiří Růžička[1,3] · Vladimír Proks[4] · Hana Macková[4] · Šárka Kubinová[1] · Dmitry Tukmachev[5] · Jiří Cihlář[6] · Daniel Horák[4] · Pavla Jendelová[1,3]

Received: 7 December 2017 / Accepted: 5 June 2018 / Published online: 25 June 2018

Abstract

While many types of biomaterials have been evaluated in experimental spinal cord injury (SCI) research, little is known about the time-related dynamics of the tissue infiltration of these scaffolds. We analyzed the ingrowth of connective tissue, axons and blood vessels inside the superporous poly (2-hydroxyethyl methacrylate) hydrogel with oriented pores. The hydrogels, either plain or seeded with mesenchymal stem cells (MSCs), were implanted in spinal cord transection at the level of Th8. The animals were sacrificed at days 2, 7, 14, 28, 49 and 6 months after SCI and histologically evaluated. We found that within the first week, the hydrogels were already infiltrated with connective tissue and blood vessels, which remained stable for the next 6 weeks. Axons slowly and gradually infiltrated the hydrogel within the first month, after which the numbers became stable. Six months after SCI we observed rare axons crossing the hydrogel bridge and infiltrating the caudal stump. There was no difference in the tissue infiltration between the plain hydrogels and those seeded with MSCs. We conclude that while connective tissue and blood vessels quickly infiltrate the scaffold within the first week, axons show a rather gradual infiltration over the first month, and this is not facilitated by the presence of MSCs inside the hydrogel pores. Further research which is focused on the permissive micro-environment of the hydrogel scaffold is needed, to promote continuous and long-lasting tissue regeneration across the spinal cord lesion.

1 Introduction

Spinal cord injury (SCI) is a devastating condition resulting in a disruption of the neuronal connections. After injury, the spinal cord lesion (SCL) develops into a combination of a pseudocystic cavity, glial and mesenchymal scar, resulting in a barrier for tissue repair and axonal regeneration [1]. Various types of experimental surgeries, that would either directly or indirectly reconstruct the lesion, have been investigated [2]. Building a bridge across the SCL using hydrogels, represents one of the therapeutic strategies in experimental SCI repair [1]. Several research groups, including ours, have shown that various hydrogels promote axonal ingrowth for a certain period of time [3–5]. Hydrogels are synthetic biomaterials providing the possibility to modify their physical and chemical properties, in order to better support and attract new tissue ingrowth inside the scaffold [4]. We can modify the chemical backbone of the scaffold, add functional groups or combine the hydrogels with other modalities, such as neurotrophic factors or stem cells [3, 4, 6, 7]. These adjustments may lead to an

✉ Aleš Hejčl
ales.hejcl@gmail.com

1 Institute of Experimental Medicine, Academy of Sciences of the Czech Republic, Vídeňská 1083, 142 20 Prague, Czech Republic

2 Department of Neurosurgery, J. E. Purkinje University, Masaryk Hospital, Sociální péče 12A, 401 13 Ústí nad Labem, Czech Republic

3 Department of Neuroscience, 2nd Faculty of Medicine, Charles University, V Úvalu 84, 150 06 Prague 5, Czech Republic

4 Institute of Macromolecular Chemistry, Academy of Sciences of the Czech Republic, Heyrovského nám.2, 162 06 Praha 6, Břevnov, Czech Republic

5 Department of Neurosurgery, Motol University Hospital, V Úvalu 84, Prague 5 150 06, Czech Republic

6 Department of Mathematics, Faculty of Science, J. E. Purkyně University, České mládeže 8, 400 96 Ústí nad Labem, Czech Republic

improved ingrowth of axons, blood vessels or connective tissue into the bridge. However, little attention has been paid to the time-dependency of tissue infiltration into the scaffold. The design of most studies utilizing scaffolds in experimental SCI repair, leads to the evaluation of the axonal ingrowth at a single time point. According to our experience with hydrogel bridging in experimental SCI, we noticed that new axons do grow inside most scaffolds during the first weeks but, when evaluated at later time points, the amount of axons seems to be rather inadequate with respect to the earlier results (unpublished data). We therefore decided to study the time-dependent dynamics of tissue ingrowth inside the scaffold.

We used SIKVAV (Ser-Ile-Lys-Val-Ala-Val)-modified highly superporous poly (2-hydroxyethyl methacrylate) (HEMA) hydrogels with oriented pores to measure the time-dependent growth of axons across the scaffold [6]. These hydrogels had a moderate modulus of elasticity, which has been shown to best promote the aligned axonal ingrowth in that study; such aligned ingrowth being convenient for the ingrowth quantification.

2 Materials and methods

2.1 Hydrogel preparation

2.1.1 Reagents

Initiator, 2,2′-azobisisobutyronitrile (AIBN; Fluka, Buchs, Switzerland), was recrystallized from ethanol. The monomers, 2-hydroxyethyl methacrylate (HEMA; Wichterle-Vacík, Prague, Czech Republic) and ethylene dimethacrylate (EDMA; Ugilor S.A., France), were purified by vacuum distillation. Ammonium oxalate and 1,4-dioxane were obtained from Lach-Ner (Neratovice, Czech Republic). 2-Aminoethyl methacrylate hydrochloride (AEMA), ɤ-thiobutyrolactone, 2,2′-dithiodipyridine, imidazole and 1,1,1,3,3,3-hexafluoro-2-propanol were from Sigma-Aldrich (St. Louis, MO, USA) and used as received. Ultrapure Q-water ultrafiltered on a Milli-Q Gradient A10 System (Millipore, Molsheim, France) was used for all experiments. HS-CGGASIKVAVS-OH peptide was synthetized according to a published procedure [8].

2.2 Preparation of poly (2-hydroxyethyl methacrylate-*co*-2-aminoethyl methacrylate) P (HEMA-AEMA) hydrogel with oriented porosity

Preparation of the hydrogel is schematically shown in Fig. 1. Briefly, freshly crystalized 30–90 µm thick and 0.3–10 mm long ammonium oxalate needles of high aspect ratio were used as a porogen for the preparation of PHEMA-based scaffolds. The ammonium oxalate crystals were parallel-oriented by shaking, which was followed by their slow sedimentation in a removable channel (12 mm in diameter) embedded in a narrow vessel on an orbital shaker (Fig. 1a). In order to maintain the crystal orientation, they were carefully transferred into the 5-ml polyethylene injection syringe with an inserted stainless sieve (32 µm), quickly washed with ethanol and dried in the air flow. The content of the crystals in the syringe was increased by the double filling of hot (90 °C) saturated oxalate solution, subsequent cooling and removing of redundant solution under vacuum (Fig. 1d). The ammonium oxalate in the syringe was then washed with ethanol and dried in an air flow and loaded with a polymerization mixture consisting of monomers (2.4 g HEMA, 0.025 g EDMA, 0.025 g AEMA), AIBN initiator (10 mg) and solvent (1,4-dioxane; 1.25 ml). The bottom of the syringe was then closed by the pressure cap and the mixture centrifuged (2000 rpm) to remove air bubbles and to homogenize the mixture. Finally, the syringe was completed with a rubber plunger and the mixture polymerized at 60 °C for 16 h. After the completion of the polymerization, the syringe was cut and the hydrogel removed (Fig. 1e). The resulting P(HEMA-AEMA) cylinder was immersed in 25% NaCl aqueous solution for 24 h to replace 1,4-dioxan and to protect the hydrogel from fast inhomogeneous swelling accompanied with hydrogel cracking. The cylinder was then transversely cut with a razor blade into discs 12 mm in diameter and 3 mm thick. Each disc was repeatedly washed with Q-water at room temperature to remove the ammonium oxalate.

2.3 Immobilization of HS-CGGASIKVAVS-OH on the P (HEMA-AEMA) discs

P(HEMA-AEMA) discs were immersed in 10 ml of aqueous 0.15 M imidazole solution and 2 ml of ethanol was added to improve the penetration of reagents in the hydrogels. 0.1 ml of ɤ-thiobutyrolactone was added under Ar and the mixture was gently shaken for 70 min. Discs were washed five times with Q-water and then transferred into 10 ml of 0.1 M phosphate buffer (pH 8) containing 3 ml of ethanol. A solution of 20 mg of 2,2′-dithiodipyridine in ethanol (2 ml) was added under Ar and the discs were incubated for 1 h. The discs were again repeatedly washed with the above described mixture of phosphate buffer and ethanol (10:3 v/v) under Ar. Finally, a solution of HS-CGGASIKVAVS-OH (2.5 mg) in 1,1,1,3,3,3-hexafluoro-2-propanol (0.25 ml) and phosphate buffer (pH 8; 6 ml) was added to the activated P(HEMA-AEMA) discs that were gently shaken for 60 min under Ar. The resulting HS-CGGASIKVAVS-modified P(HEMA-AEMA) discs were washed five times with Q-water, sterilized in 70% ethanol for 16 h and transferred in sterile 100-ml bottles.

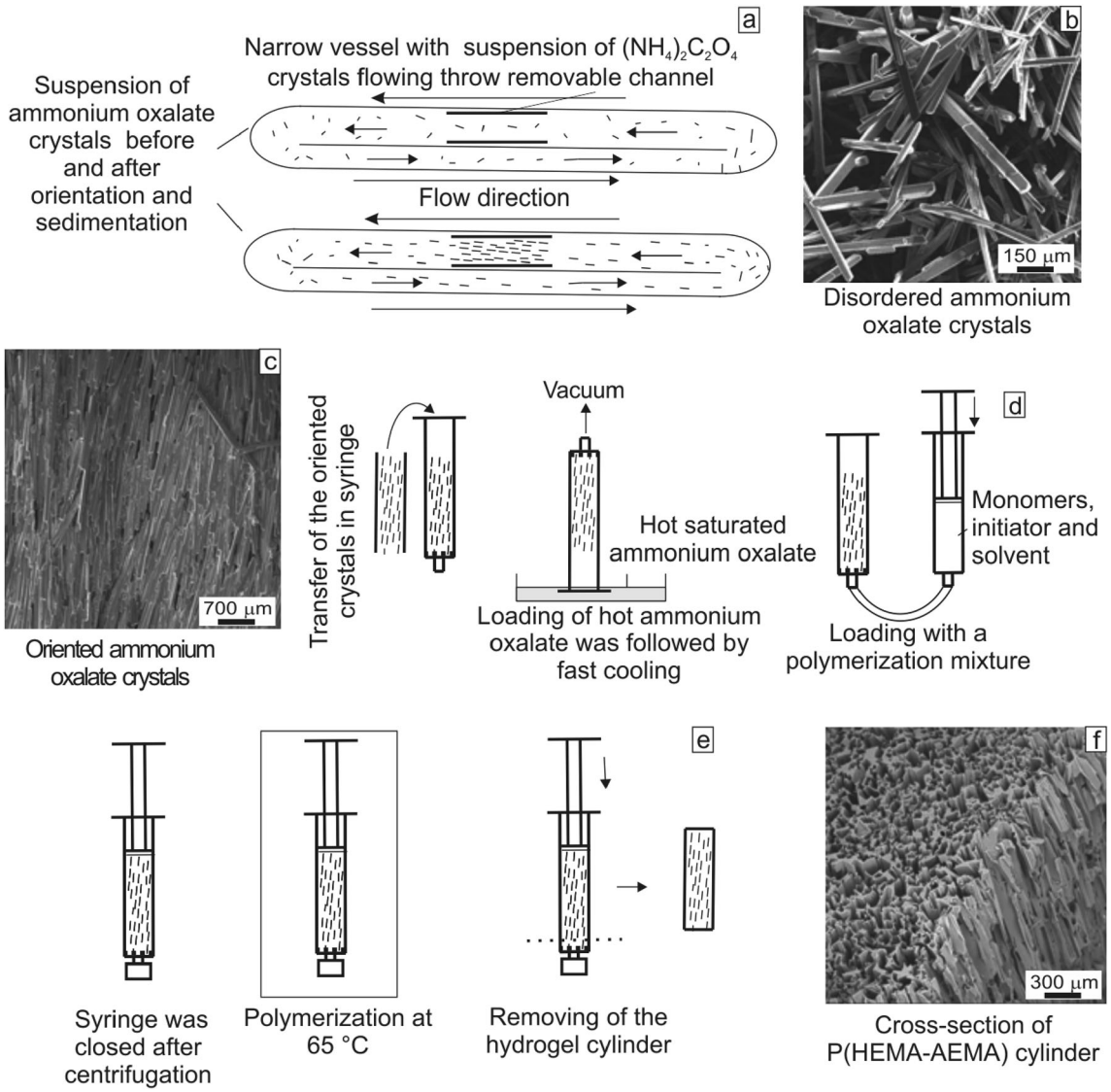

Fig. 1 Scheme of preparation of P(HEMA-AEMA) hydrogel. **a** Orientation of ammonium oxalate needles. SEM micrographs of **b** disorder and **c** oriented crystals. **d** Transfer of crystals and polymerization mixture to the syringe. **e** Preparation of P(HEMA-AEMA) cylinder. **f** SEM micrograph of P(HEMA-AEMA) hydrogel with oriented porosity

2.4 Characterization

P(HEMA-AEMA) discs were analyzed by a JSM 6400 scanning electron microscope (SEM; Jeol; Tokyo, Japan). The samples were sputter-coated with 4 nm Pt before imaging. The immobilization HS-CGGASIKVAVS-OH was indirectly determined by the observation of UV spectra of 2-thiopyridine, measured with a Lambda 20 spectrometer (Perkin-Elmer; Norwalk, CT, USA). Pascal 140 and 440 mercury porosimeter (ThermoFinigan; Rodano, Italy) was used for measuring the average pore size of the dry hydrogels in two pressure intervals, 0–400 kPa and 1–400 MPa [9]. A specific surface area of the dried hydrogels was measured by nitrogen adsorption, using a Gemini VII 2390 Analyzer (Micromeritics; Norcross, USA) at 77 K.

2.5 Seeding of MSCs on hydrogels

To enable the more easily distinguishable and stable tracking of the transplanted cells, rat MSCs expressing enhanced green fluorescent protein (GFP) isolated from GFP+ rats, were used in our experiments. The transgenic Sprague–Dawley rats [SD-Tg(CAG-EGFP)CZ-004Osb] were kindly provided by Dr. Masaru Okabe (Osaka University, Japan) [10], bred at the laboratory of Dr. Martin Marsala (University of California, San Diego, CA), then subsequently sent to our Institute, and bred in our animal facility.

The cells were isolated by extrusion of the bone marrow into a tissue culture Petri dish. The cells were plated in DMEM/10% fetal bovine serum with primocin (2 ml/ml). After 24 h, the non-adherent cells were removed by replacing the medium. When cells reached 75%–90% confluence, they were detached by trypsin/EDTA treatment and transferred into 75-cm^2 cell culture flasks. MSCs from passage 3 were used for in vitro and in vivo experiments. On the day of the hydrogel seeding, the cultures were trypsinized with a 0.25% trypsin/ethylenediaminetetraacetic acid (EDTA) solution. Two million cells per milliliter were then placed in a test tube along with a 2 × 2 × 2 mm cube of hydrogel and put on a shaker (500 rpm) for 15 min in order to seed the 3D scaffold. We performed no quantitative analysis regarding the actual amount of seeded cells. However, our earlier study showed that the HEMA hydrogel provides good affinity to MSCs [4]. The hydrogels were implanted within 3 h after seeding.

2.6 Animal handling and surgery

This study was performed in accordance with the European Communities Council Directive of 22nd of September 2010 (2010/63/EU) regarding the use of animals in research, and was approved by the Ethics Committee of the Institute of Experimental Medicine, Academy of Sciences of the Czech Republic.

2.7 Spinal cord transection

Forty-six male rats (Wistar, Anlab, Czech Republic) with a weight of 300–350 g, underwent transection at the Th8 level. The animals were intraperitoneally injected with pentobarbital for anesthesia (0.06 g/1 kg i.p.); one dose of ATB (gentamicin 8 mg/1 kg i.m.), atropine (0.08 mg/1 kg s.c.), and mesocain to enhance local anesthesia (1 mg/1 kg s.c. + i.m.) was administered preoperatively. In addition, the rats received cyclosporine (Novartis; 10 mg/kg i.p.) before surgery and then daily until sacrifice. A linear skin incision was performed above the spinous processes of Th7-9; the paravertebral muscles were detached from the laminae Th7-9, and a Th8 laminectomy was performed. The dura was incised longitudinally in the midline and about a 2 mm-segment of spinal cord was dissected, creating a cavity resulting in complete spinal cord transection. The size and the character of the lesion were identical to our earlier study [11].

2.8 Hydrogel implantation

One week after the transection, we reopened the scar tissue from the skin to the spinal cord. We extracted the suture from the dura and removed the debris from the lesion. The hydrogels were properly trimmed to adjust to the size and shape of the cavity. The hydrogel was taken from the EDTA solution and implanted wet in such a way as to ensure that it would firmly adhere to the edges of the transection cavity without causing any undue pressure onto the surrounding spinal cord tissue. Such approach ensures no further swelling of the hydrogel within the cavity. The muscles and skin were sutured again, and the animals were housed two in a cage with food and water ad libitum. The number of animals in each group regarding therapy (hydrogel with or without MSCs) and timing are summarized in Table 1.

Table 1 Numbers of experimental animals

Days after hydrogel implantation	2	7	14	28	49	168
SIKVAV-HEMA	3	3	3	4	3	0
SIKVAV-HEMA with MSCs	3	4	5	6	3	3
Total	6	7	8	10	6	3

2.9 Retrograde staining

Six months after SCI, under isoflurane anesthesia, a laminectomy of the lumbar vertebra 12 and 13 was performed and 2 µl of 2% hydroxystilbamidine (Fluorogold, Invitrogen, Carlsbad, CA) were stereotactically injected by a Nano-Injector (Stoelting Co., Wood Dale, IL) into the dorsal columns of 5 animals treated with hydrogel and MSCs. Two days later, the animals were perfused transcardially with phosphate-buffered saline (PBS) followed by 4% paraformaldehyde.

Sections were first incubated with anti-fluorogoldantibody (1:10,000; Chemicon International, Temecula, CA) then with biotinylated goat anti-rabbit secondary antibody (1:1000; Vector Labs, Burlingame, CA). They were processed using Vectastain ABC reagent (Vector Labs) and developed with diaminobenzidine (Vector Labs).

2.10 Tissue processing and histology

The animals were sacrificed 2, 7, 14, 28, 49 days and 6 months after hydrogel implantation. They were then deeply anesthetized with an intraperitoneal injection of overdose pentobarbital and perfused with physiological saline, followed by 4% paraformaldehyde in 0.1 M phosphate buffer. The spinal cord was left in the bone overnight, then removed and postfixed in the same fixative for at least 1 week.

A 4 cm-long segment of the spinal cord with the lesion site in the middle was dissected, and a series of 40 mm-thick longitudinal sections were collected. Hematoxylin–eosin staining was performed, using standard protocols, and the

slides were specifically evaluated using an Axio Observer D1 microscope (Carl Zeiss MicroimagingGmbH). For immunohistochemical studies, the following primary antibodies and dilutions were used: Cy3-conjugated anti-GFAP (1:200; Sigma-Aldrich) to identify astrocytes, anti-NF 160 (1:200; Sigma-Aldrich) to identify neurofilaments, and RECA-1 (1:50; Abcam) to identify endothelial cells of blood vessels. Alexa Fluor 594 goatanti–rabbit IgG (1:200; Invitrogen) and Cy3-conjugated anti-mouseIgM (1:100; Invitrogen) were used as secondary antibodies.

2.11 Tissue quantification

For each spinal cord, 4 to 5 slices were used for the quantification of axons. The hydrogels were divided into 3 parts: the cranial end, the central part and the caudal end. We calculated the number and the length of axons in each part of the scaffold, using the program Tissue Quest Analysis Software (Tissue Gnostics GmbH, Vienna, Austria). We then combined the data from the peripheral parts of the hydrogels (cranial and caudal ends) and evaluated them together. The central part was quantified and analyzed separately.

Blood vessels were evaluated via a semi-quantitative method using 4 slices for each spinal cord, as described in our previous paper [4]. We analyzed the number of green objects, regardless of the size of each object (number of areas), the total number of the green objects (sum of areas), and the intensity of the green color on each slice (densitometry) using Axio Vision 4.8 software (Carl Zeiss Microimaging GmbH, Jena, Germany). However, when the shape of the object was obviously not a blood vessel, it was manually excluded in order to avoid counting artifacts. By multiplying the "sum of areas" and the "densitometry" parameters, we obtained a semi-quantitative parameter, directly related to the number of blood vessels in the hydrogel *in vivo*.

The mean values are reported as mean ± SEM. Intergroup differences were analyzed using ANOVA,

and a Student's two-sample t-test (probability values <0.05 and <0.01 were considered statistically significant).

3 Results

3.1 Hydrogel scaffolds

Non-degradable PHEMA scaffolds were prepared by the radical polymerization of HEMA, EDMA and AEMA in the presence of a porogen-ammonium oxalatein small polyethylene syringes by a modification of the earlier described procedure [6]. The resulting hydrogel cylinders were subsequently cut on discs. The advantage of polymerization in the syringes, consists mainly in minimizing contact of the hydrogel surface with the polymerization mold which could induce inhomogeneity of the hydrogel at the interface. A low concentration of EDMA (1 wt.%) was used to afford good mechanical properties of the hydrogel. Reactive amino groups were introduced by copolymerization of the monomers with 1 wt.% AEMA. To produce continuous pores in the hydrogel, which are required for the ingrowth of axons when implanted in the damaged spinal cord, it is necessary to orient the $(NH_4)_2C_2O_4$ crystals by gentle shaking on an orbital shaker. Figure 1b,c shows the $(NH_4)_2C_2O_4$ crystals before and after the orientation. The advantage of the $(NH_4)_2C_2O_4$ crystals consists in their needle-like shape, which in contrast to conventional porogens, such as cubic NaCl [12] or sucrose [13], provides connectivity between the pores and also enables a high level of filling due to the ordered crystal structure. Moreover, a double loading of saturated $(NH_4)_2C_2O_4$ solution raised crystal content in the syringe, as the crystals/cylinder volume ratio increased from 0.52 to 0.75. The SEM micrograph of a cross-section of the P(HEMA-AEMA) hydrogel, demonstrated that the orientation of the crystals during loading remained unchanged and a hydrogel with continuous pore channels was obtained after completion of the polymerization (Fig. 1e). The pore size (SEM) was identical to that of the original crystals, i.e., ~60 µm in diameter and a few mm in length. Mercury porosimetry confirmed the 70 µm pore size in the dry hydrogels. The large specific surface area of the P(HEMA-AEMA) hydrogel (82 m^2/g), determined by BET isotherm, documented the presence of macropores (<1 µm) in the polymer which could be beneficial for the prospective sufficient nourishment of the cells. In order to support cell adhesion, the P(HEMA-AEMA) hydrogel was coated with HS-CGGASIKVAVS-OH peptide. Its immobilization on the polymer surface was indirectly indicated by measuring the UV spectra of solutions before and after the reaction. Figure 2a shows characteristic adsorption bands of 2-thiopyrine in the spectrum at 272 and 337 nm, indicating 2-thiopyrine release from the activated P(HEMA-AEMA) discs in the supernatant after the reaction with peptide. After seeding MSCs attached and spread mostly parallel to the oriented pores of the hydrogels (2B).

3.2 Bridging the post-traumatic cavity with hydrogels

During the hydrogel manipulation and implantation, the scaffold was soft enough to adjust the shape and size of the post-transection cavity. The hydrogels bridged the transection cavity adequately. They adhered well to the spinal cord with minimal or no pseudocystic cavities. There was also no progression of pseudocystic cavities observed in time.

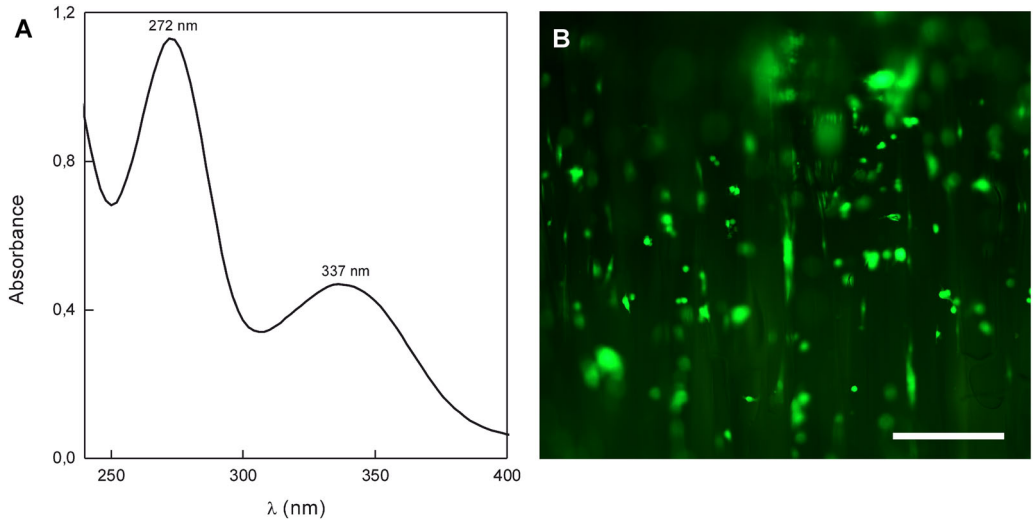

Fig. 2 **a** UV-spectrum of 2-thiopyridine released after immobilization of Ac-CGGASIKVAVS-OH on activated P(HEMA-AEMA) hydrogel. **b** MSCs attached to the hydrogel, many of them oriented along the pores of the scaffold

There were no signs of foreign body reactions observed in or around the hydrogels, either in the early or later stage after hydrogel implantation.

3.3 Connective tissue infiltration of the hydrogel scaffolds

Two days after hydrogel implantation, the pores of the hydrogels were dominantly filled with blood cells (Fig. 3a). There were no connective tissue elements observed in the pores, just a few myofibrils growing in the border zones of both groups of animals treated with hydrogels (with or without MSC). One week after hydrogel implantation, connective tissue elements infiltrated the whole volume of the hydrogel, both the periphery as well as the central part (Fig. 3b). MSCs were present in the pores of the hydrogel within the whole period, as long as 6 months after SCI (Fig. 3c). There was no difference in the amount of connective tissue between hydrogels seeded with MSC and without MSC. Also, we observed no change in the amount of connective tissue in the peripheral and central parts of the hydrogels from week 1 to week 7 after hydrogel implantation (Fig. 4).

3.4 Dynamics of axonal infiltration

Two days after hydrogel implantation, no axons were found either in the periphery or in the central part of the hydrogel. One week after hydrogel implantation, a few axons grew into the peripheral parts (mean total length = 71 ± 83 µm) with none growing any further into the central part of the scaffold (Fig. 3d). Two weeks after hydrogel implantation, the number of axons grew significantly (mean total length = 188 ± 76 µm) into the peripheral parts of the hydrogel scaffold. The neural sprouts grew further and infiltrated the central parts of the hydrogel (mean total length = 96 ± 57 µm). Four weeks after hydrogel implantation, the neural sprouts continued to infiltrate the peripheral part (mean total length = 344 ± 160 µm). The axons also grew further into the central part of the scaffold with the mean total length of the axons 134 ± 80 µm. Seven weeks after the hydrogel implantation we observed a rather stable number of axons in the peripheral part with no further increase, compared to 4 weeks after implantation (mean total length = 327 ± 153 µm), while in the central part the number of axons was 171 ± 124 µm (Fig. 5).

Axons infiltrated the pores of the hydrogel in a slower and more gradual manner. Overall, they infiltrated about 2–4% of the whole volume of the scaffold in the peripheral parts and about 1.5–2% in the central part, guided in the cranio-caudal or caudo-cranial direction by the oriented pores of the hydrogel (Fig. 3e).

When we compared the axonal infiltration of hydrogels or hydrogels seeded with MSCs, we found no statistically significant difference between both groups at any time point, both in the peripheral as well as in the central parts of the hydrogel.

3.5 Dynamics of blood vessels ingrowth

There were no blood vessels in the scaffold 2 days after implantation, but the peripheral as well as the central parts of the hydrogels were filled with blood cells. The first blood vessels started to grow into the peripheral part of the hydrogels 1 week after implantation (Fig. 3f). However, the number of blood vessels did not increase between day 7 and

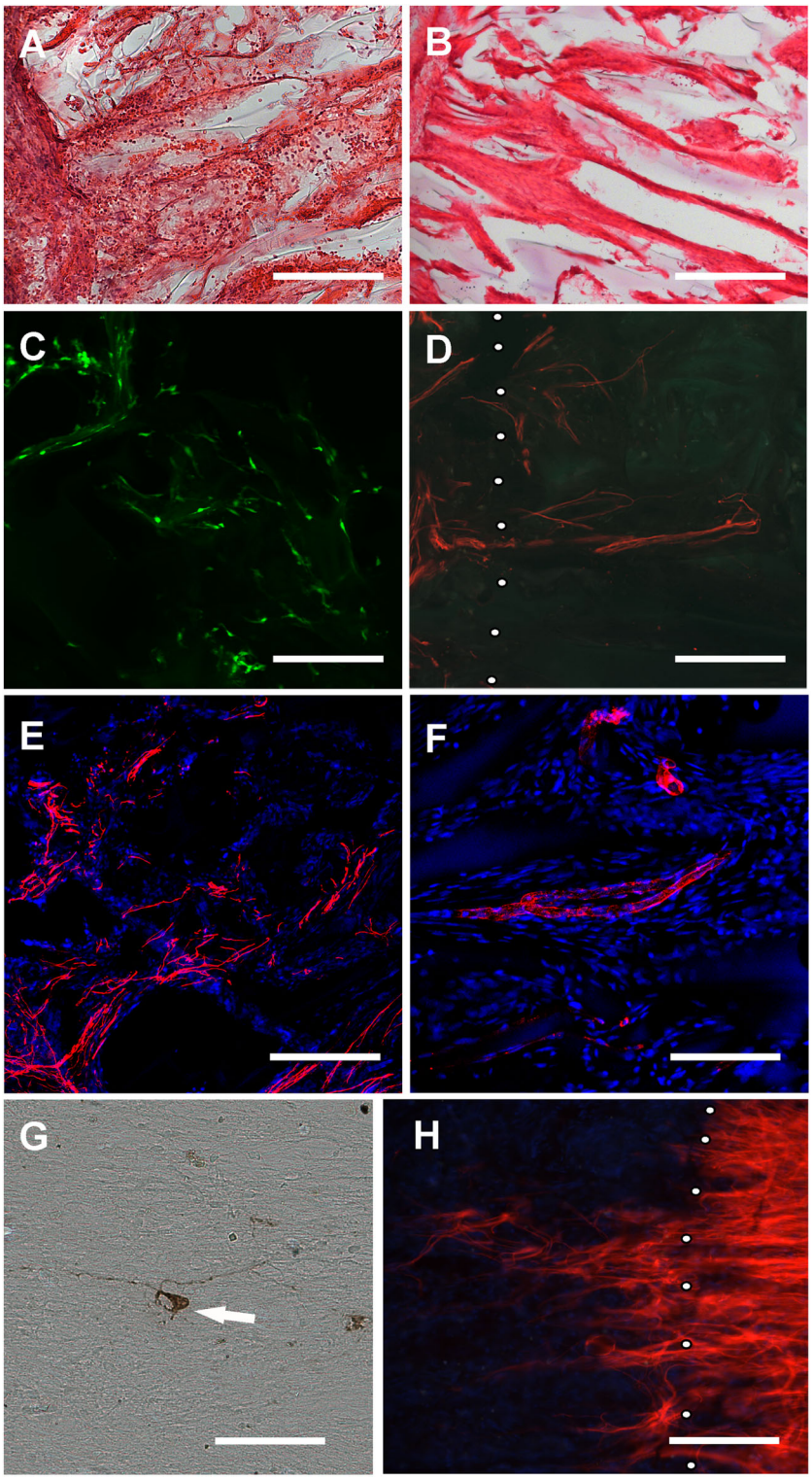

Fig. 3 SIKVAV-HEMA scaffolds bridging a posttraumatic cavity after spinal cord transection. **a** Left border region of the HEMA hydrogel 2 days after implantation in SCI. The pores are filled with blood elements, without any connective tissue (HE staining, scale bar = 100 µm). **b** One week after implantation of the HEMA scaffold the pores are completely filled with connective tissue (HE staining, scale bar = 100 µm). **c** GFP-positive MSCs 6 months after implantation of the HEMA scaffold seeded with MSCs (GFP staining, scale bar = 50 µm). **d** Neural sprouts invading pores of the bordering zone of the HEMA scaffold 2 weeks after implantation (NF160-g594 immunostaining, scale bar = 100 µm). **e** Axons in the central part of the HEMA scaffold seeded with MSCs 7 weeks after implantation are directed through the pores predominantly in the cranio-caudal or caudo-cranial direction (NF160-g594 immunostaining, scale bar = 100 µm). **f** Blood vessels infiltrating the pores of the HEMA scaffold (RECA-g594 immunostaining, scale bar = 100 µm). **g** Rare neurons were found to be fluorogold-positive in the spinal cord cranial from the tissue-scaffold border (white arrow, fluorogold staining, scale bar = 25 µm). **h** Astrocytes invading the peripheral part of the HEMA-scaffold 6 months after implantation (GFAP-Cy3, scale bar = 100 µm)

days 14, 28 or 49 and it became rather static until day 49 after SCI (Fig. 6). There were no statistically significant differences in the number of blood vessels observed during that time period. The blood vessels grew into the peripheral area and the same amount grew into the central parts of the hydrogel (Fig. 5).The same dynamics in the growth of blood vessels was observed in the hydrogels seeded with MSCs. We observed no statistically significant difference in the number of MSC between plain hydrogels and hydrogels seeded with MSCs.

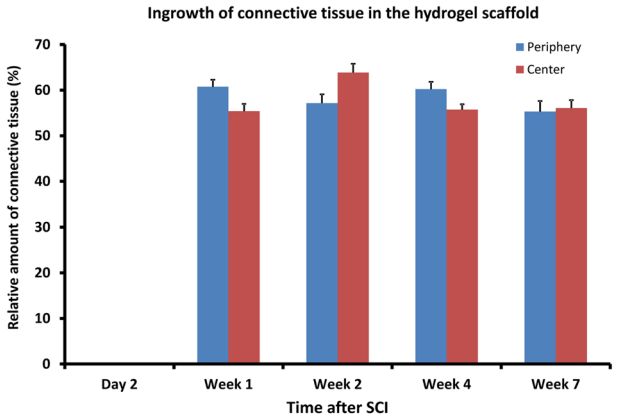

Fig. 4 Dynamics of connective tissue infiltration in the SIKVAV-HEMA scaffolds

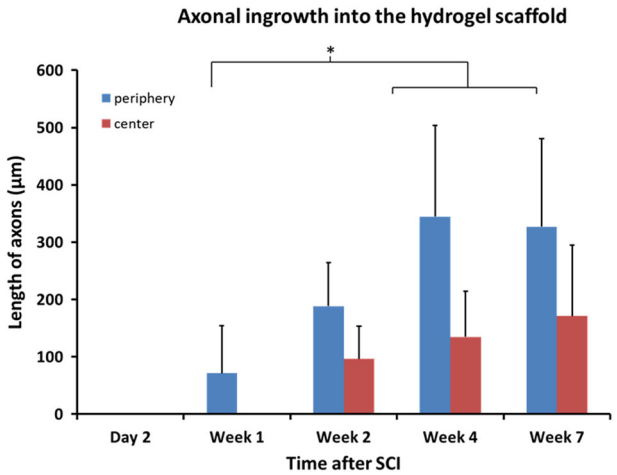

Fig. 5 Dynamics of axonal ingrowth in the SIKVAV-HEMA scaffold. A statistically significant increase in the number of axons is apparent between Day 7 and Weeks 4 and 7 after hydrogel implantation (*$p < 0.05$). There is a gradual increase in the number of axons infiltrating the scaffold

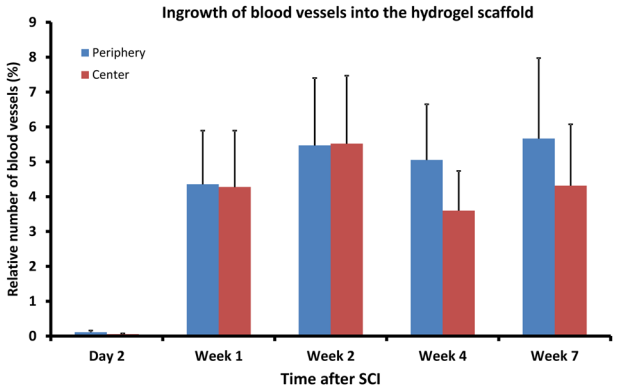

Fig. 6 Blood vessel ingrowth in the SIKVAV-HEMA scaffolds

3.6 Long-term results

Three rats were sacrificed 6 months after SCI. These were treated with hydrogels seeded with MSCs. MSCs were still abundantly present in the hydrogel scaffold 6 months after implantation (3 C). Six months after hydrogel implantation, most axons stopped at the tissue-hydrogel border, while some entered the hydrogel. We found only scarce positively-stained fluorogold neurons with projections in the cranial part of the spinal cord (Fig. 3g). In comparison to the early stage, we found that several astrocytes crossed into the hydrogel scaffold (Fig. 3h), however, their processes did not populate the hydrogel center.

4 Discussion

Complete SCI leads to disruption of the spinal cord tracts resulting in the formation of a pseudocystic cavity, glial and mesenchymal scar [14]. Implanting a hydrogel scaffold inside the post-traumatic cavity, represents one of the experimental approaches to reconstruct the spinal cord lesion [11]. Despite some progress, we have not yet achieved a complete bridging of the lesion with abundant axons crossing the barrier and forming functional connections. To do this, we would need to create an environment that would promote extensively progressive ingrowth of axons into and out of the hydrogel scaffold. However, no study has yet focused on the dynamics of tissue ingrowth into the hydrogel after implantation inside the spinal cord lesion.

In our previous research, we evaluated various types of hydrogel scaffolds [3, 4, 6, 7, 11, 15, 16] and noticed that after a few weeks of progressive ingrowth of axons, the results seemed rather disappointing in the long-term. We, therefore, decided to study the time-related ingrowth of axons into a hydrogel scaffold, using a SIKVAV-modified superporous PHEMA hydrogel with oriented pores. In our earlier study we found that moderate elastic modulus and porosity in these PHEMA scaffolds, showed a good combination of bridging properties, tissue infiltration and abundant axonal ingrowth [8]. Furthermore, we have shown that the oriented pores gave directed axonal guidance in the cranio-caudal and caudo-cranial direction, which allows an easy evaluation of the amount and the length of axons into the scaffold. We also seeded one group of the hydrogels with MSCs in order to assess whether these commonly used stem cells provide any advantage for the ingrowth of axons or blood vessels over time.

The hydrogels were implanted in a spinal cord transection cavity. This kind of experimental lesion mimics the most severe type of clinical SCI, in which the tissue is physically completely torn. Patients with complete spinal

cord injury (ASIA A) would be among the first to be included in clinical trials where the spinal cord lesion would be reconstructed utilizing non-injectable scaffolds, as there is no risk of losing any residual function [17]. At the same time, such an operation would be performed after some delay from the moment of injury, as the indication and the inclusion process require some time. We performed the implantation after a one week delay respecting the necessary time window. As we had also shown previously, such an approach may be even better than immediate surgery, as it improves adhesion to the edges of the spinal cord while minimizing the development of post-traumatic cavities [11].

4.1 Axonal growth into the hydrogel scaffold

The SIKVAV-HEMA-based hydrogel scaffold provided a permissive environment for the ingrowth of connective tissue, blood vessels and most importantly axons. While the ingrowth of connective tissue was rather fast, as it completely infiltrated the pores within the first week, axons infiltrated the scaffold in a slower and more gradual manner. The hydrogel scaffold attracted new axonal ingrowth but only for a limited period of time. Several factors could be considered to cause such a time-limited infiltration of the hydrogel scaffolds. One reason could be the spatial limitation in the hydrogel pores, due to the connective tissue infiltration. However, we demonstrated in our study that the connective tissue already fills the hydrogel pores within the first week, then remains stable for the next 2 months. However, the axons continued to grow progressively into the pores of the hydrogel during the first month after implantation. Therefore, the space limitation does not seem to be the decisive factor.

Another possible reason could be the lack of nutrients and growth factors in the hydrogel over time. We seeded some of our hydrogels with MSCs. MSCs may promote lesion repair and prevent neuronal apoptosis by secreting growth factors, such as the BDNF (brain-derived neurotrophic factor), VEGF (vascular endothelial growth factor), the NGF (nerve growth factor) or the GDNF (glial-derived neurotrophic factor) [18]. Furthermore, MSCs promote CNS plasticity [19]. In this study, however, we did not find any improvement in the number or in the growth dynamics of axons when the hydrogels were seeded with MSCs. Some other studies came to the same conclusion [20]. We showed that many MSCs were present within the scaffold as long as 6 months after SCI. Nonetheless, the number of present cells does not necessarily correlate with the extent of their metabolic activity [21]. Also, many groups, including ours, have shown neuroprotective and tissue preservation abilities of MSCs rather their influence on increased ingrowth of neural sprouts within the scaffold [3, 22, 23]. Using plain MSCs may be insufficient, but by creating genetically engineered MSCs overexpressing some of the growth factors (BDNF or VEGF), we may achieve improved tissue repair including the promotion of axonal ingrowth [24]. The effect of MSCs also seems be facilitated by adding other supportive cells, e.g. Schwann cells [25]. For this reason, MSCs modifications may promote their positive effect on the neuronal repair after SCI.

One of the important factors is the micro-environmental milieu of the scaffold. The inner architecture of the hydrogel is one of the key components of the micro-environmental milieu. The inner structure is determined by the physical and chemical properties of the scaffold. In one of our previous studies, we found that the web-like architecture of the hydrogel, together with the HPMA-based backbone of the hydrogel, promotes the ingrowth of new axons despite promoting the adhesion of fewer MSCs compared to HEMA-based hydrogels [4]. The data from these two studies, suggests that the effect of MSCs seeded on hydrogels is less important than the inner milieu of the hydrogel, influenced by the chemical backbone and the architecture of the scaffold.

We also utilized a SIKVAV sequence attached to the hydrogels to promote cellular adhesion and growth-promoting properties. The SIKVAV sequence, a synthetic peptide from active regions of the A chain of basement membrane laminin, promotes cell adhesion and neural outgrowth by the binding of transmembrane integrin receptors [26]. The positive effect of the SIKVAV sequence on axonal regeneration and functional outcome sequence has been demonstrated previously [27, 28]. In one of our previous studies, PHEMA-based scaffolds modified with the SIKVAV sequence, promoted in vitro cell adhesion and axonal regeneration [8]. However, it still seems inadequate for a long-time promotion of axonal ingrowth. Therefore, the question remains of how to ensure long-term survival and promotion of axons in the hydrogel scaffolds. One of the strategies for axonal growth is the genetic manipulation of the injured axons. For migration, axonal growth cones require an adhesion complex that signals and links to the cytoskeleton. Integrins can belong to the targeted adhesion molecules, because axons regenerating through the CNS, particularly the scar tissue, must penetrate the extracellular matrix (ECM) for which integrins are the main receptors. Integrins, particularly $\alpha 9\beta 1$, are expressed in the CNS and PNS in embryogenesis, then downregulated and not re-expressed after injury [29]. Fawcett's group was able to obtain very extensive long-distance sensory axon regeneration in the spinal cord, by transducing sensory neurons with a tenascin-binding integrin and an integrin activator [30]. Our hydrogels can have different peptide sequences bound to the surface; however, the axons are not able to fully utilize the signals due to the missing integrin subunits. Therefore the potential of biomimetic materials can be

facilitated by modifying the axons to express a growth-promoting receptor for the matching sequence.

Another approach to promote the long-term growth and stability of axons, is to create a continuous milieu of trophic factors, such as the combination of olfactory ensheathing cells (OEC), together with olfactory nerve fibroblasts injected into the hydrogel scaffold, and with injections both in the rostral and caudal ends of the adhering spinal cord [31]. This leads to the promotion of cortico-spinal axons rostral to the lesion, but not across the lesion [32]. In a later study, a scaffold with guiding mini-channels seeded with GDNF-overexpressing Schwann cells, resulted in the growth of propriospinal axons across a bridge, their regeneration, formation of synapses and partial functional recovery [33].

4.2 Neovascularization in the hydrogel scaffold

Neovascularization at the site of the injury may provide oxygen and nutrition for axonal regeneration. Promoting the ingrowth of vasculature, may lead to improved axonal regrowth and functional recovery [34, 35]. Therefore manipulating the endogenous response towards promoting vascular repair is a logical step in tissue engineering. Our study showed that the blood vessels started to grow a few days after the lesion and were found not only in the peripheral part, but already grew long enough into the central part of the hydrogel 7 days after the SCI. However, there was no significant increase in the amount of blood vessels after the first week. This study also shows that the presence of MSCs does not increase the ingrowth of new blood vessels into the hydrogel scaffold, although many studies have shown that MSCs induce angiogenesis in injured tissues [36]. It is promoted by the paracrine release of the VEGF [37]. We have shown previously that new blood vessels often grow into the pores of the scaffold in close proximity to MSCs seeded in hydrogel scaffolds [3].

Various adhesion promoting approaches have been applied to promote angiogenesis [4, 38]. In one of our former studies, we found that the RGD peptide sequence promotes vascular growth into the hydrogel scaffolds when implanted in a spinal cord lesion [4]. The exogenous growth factors (GF) usually need to be applied at the site of injury in a supraphysiological level as they degrade quickly. Conversely, the tissue itself reacts to injury by increasing the levels of the vascular endothelial growth factor (VEGF) and the implantation of biomaterials activates the secretion of several cytokines [39, 40]. Feng et al. therefore propose taking advantage of such endogenous processes [41]. Using properly engineered injectable hydrogels, they activated macrophages to secrete pro-angiogenic cytokines, and released endogenous angiogenesis promoting growth factors inside the hydrogel. The manipulation with growth factors seems to be a stronger pro-angiogenetic tool than the presence of MSCs.

5 Conclusions

After hydrogel implantation inside a spinal cord lesion, the pores of the SIKVAV-HEMA scaffold are completely filled with connective tissue elements within the first week. Also, blood vessels infiltrate about 5% of the total hydrogel volume within the first week and the amount stays stable for the next 2 months. Axons, on the other hand, infiltrate the hydrogel scaffold in a gradual manner. The amount progresses within the first 4 weeks in the hydrogel scaffold and then remains stable. Rare axons were found to cross the bridge into the distal stump of the spinal cord. MSCs did not show any effect on the hydrogel infiltration over time with respect to the speed or the amount of any tissue infiltration. We need to investigate modifications and additional therapies that would enable long-time progressive infiltration of axons into the scaffold, which would be sufficient enough to cross the bridge and create new synapses leading to functional restoration.

Acknowledgements We would like to thank Frances Zatřepálková and Jan Lodin for proofreading the manuscript. The study has been supported by 2 grants from the Grant Agency of the Czech Republic 14-14961S, 17-11140S, the Operational Programme Research, Development and Education in the framework of the project "Centre of Reconstructive Neuroscience ", registration number CZ.02.1.01/0.0./0.0/15_003/0000419 and by the grant from the Ministry of Education, Youth and Sports No. LO1309.

Compliance with ethical standards

Conflict of interest The authors declare that they have no conflict of interest.

References

1. Geller HM, Fawcett JW. Building a bridge: engineering spinal cord repair. Exp Neurol. 2002;174:125–36. https://doi.org/10.1006/exnr.2002.7865.
2. Hejčl AJ, Sameš P, Syková M. Experimental treatment of spinal cord injuries. Cesk Slov Neurol N. 2015;78/111:377–93.
3. Hejcl A, Sedy J, Kapcalova M, Toro DA, Amemori T, Lesny P, et al. HPMA-RGD hydrogels seeded with mesenchymal stem cells improve functional outcome in chronic spinal cord injury. Stem Cells Dev. 2010;19:1535–46. https://doi.org/10.1089/scd.2009.0378.
4. Hejcl A, Ruzicka J, Kapcalova M, Turnovcova K, Krumbholcova E, Pradny M, et al. Adjusting the chemical and physical properties of hydrogels leads to improved stem cell survival and tissue ingrowth in spinal cord injury reconstruction: a comparative study of four methacrylate hydrogels. Stem Cells Dev. 2013;22:2794–805. https://doi.org/10.1089/scd.2012.0616.

5. Nomura H, Baladie B, Katayama Y, Morshead CM, Shoichet MS, Tator CH. Delayed implantation of intramedullary chitosan channels containing nerve grafts promotes extensive axonal regeneration after spinal cord injury. Neurosurgery. 2008;63:127–41. https://doi.org/10.1227/01.NEU.0000335080.47352.31.
6. Kubinova S, Horak D, Hejcl A, Plichta Z, Kotek J, Proks V, et al. SIKVAV-modified highly superporous PHEMA scaffolds with oriented pores for spinal cord injury repair. J Tissue Eng Regen Med. 2015;9:1298–309. https://doi.org/10.1002/term.1694.
7. Hejcl A, Lesny P, Pradny M, Sedy J, Zamecnik J, Jendelova P, et al. Macroporous hydrogels based on 2-hydroxyethyl methacrylate. Part 6: 3D hydrogels with positive and negative surface charges and polyelectrolyte complexes in spinal cord injury repair. J Mater Sci Mater Med. 2009;20:1571–7. https://doi.org/10.1007/s10856-009-3714-4.
8. Kubinova S, Horak D, Kozubenko N, Vanecek V, Proks V, Price J, et al. The use of superporous Ac-CGGASIKVAVS-OH-modified PHEMA scaffolds to promote cell adhesion and the differentiation of human fetal neural precursors. Biomaterials. 2010;31:5966–75. https://doi.org/10.1016/j.biomaterials.2010.04.040.
9. Salek P, Korecka L, Horak D, Petrovsky E, Kovarova J, Metelka R, et al. Immunomagnetic sulfonated hypercrosslinked polystyrene microspheres for electrochemical detection of proteins. J Mater Chem. 2011;21:14783–92. https://doi.org/10.1039/c1jm12475g.
10. Okabe M, Ikawa M, Kominami K, Nakanishi T, Nishimune Y. 'Green mice' as a source of ubiquitous green cells. FEBS Lett. 1997;407:313–9.
11. Hejcl A, Urdzikova L, Sedy J, Lesny P, Pradny M, Michalek J, et al. Acute and delayed implantation of positively charged 2-hydroxyethyl methacrylate scaffolds in spinal cord injury in the rat. J Neurosurg Spine. 2008;8:67–73. https://doi.org/10.3171/SPI-08/01/067.
12. Horák D, Hradil H, Lapčíková M, Šlouf M. Superporous poly(2-hydroxyethyl methacrylate) based scaffolds: preparation and characterization. Polymer. 2008;49:2046–54.
13. Horak D, Kroupova J, Slouf M, Dvorak P. Poly(2-hydroxyethyl methacrylate)-based slabs as a mouse embryonic stem cell support. Biomaterials. 2004;25:5249–60. https://doi.org/10.1016/j.biomaterials.2003.12.031.
14. Fitch MT, Doller C, Combs CK, Landreth GE, Silver J. Cellular and molecular mechanisms of glial scarring and progressive cavitation: in vivo and in vitro analysis of inflammation-induced secondary injury after CNS trauma. J Neurosci. 1999;19:8182–98.
15. Ruzicka J, Romanyuk N, Hejcl A, Vetrik M, Hruby M, Cocks G, et al. Treating spinal cord injury in rats with a combination of human fetal neural stem cells and hydrogels modified with serotonin. Acta Neurobiol Exp. 2013;73:102–15.
16. Hejcl A, Lesny P, Pradny M, Michalek J, Jendelova P, Stulik J, et al. Biocompatible hydrogels in spinal cord injury repair. Physiol Res. 2008;57(Suppl 3):S121–32.
17. Amr SM, Gouda A, Koptan WT, Galal AA, Abdel-Fattah DS, Rashed LA, et al. Bridging defects in chronic spinal cord injury using peripheral nerve grafts combined with a chitosan-laminin scaffold and enhancing regeneration through them by co-transplantation with bone-marrow-derived mesenchymal stem cells: case series of 14 patients. J Spinal Cord Med. 2014;37:54–71. https://doi.org/10.1179/2045772312Y.0000000069.
18. Li N, Sarojini H, An J, Wang E. Prosaposin in the secretome of marrow stroma-derived neural progenitor cells protects neural cells from apoptotic death. J Neurochem. 2010;112:1527–38. https://doi.org/10.1111/j.1471-4159.2009.06565.x.
19. Hao P, Liang Z, Piao H, Ji X, Wang Y, Liu Y, et al. Conditioned medium of human adipose-derived mesenchymal stem cells mediates protection in neurons following glutamate excitotoxicity by regulating energy metabolism and GAP-43 expression. Metab Brain Dis. 2014;29:193–205. https://doi.org/10.1007/s11011-014-9490-y.
20. Gunther MI, Weidner N, Muller R, Blesch A. Cell-seeded alginate hydrogel scaffolds promote directed linear axonal regeneration in the injured rat spinal cord. Acta Biomater. 2015;27:140–50. https://doi.org/10.1016/j.actbio.2015.09.001.
21. Oliveira E, Assuncao-Silva RC, Ziv-Polat O, Gomes ED, Teixeira FG, Silva NA, et al. Influence of different ECM-like hydrogels on neurite outgrowth induced by adipose tissue-derived stem cells. Stem Cells Int. 2017;2017:6319129 https://doi.org/10.1155/2017/6319129.
22. Papa S, Vismara I, Mariani A, Barilani M, Rimondo S, De Paola M, et al. Mesenchymal stem cells encapsulated into biomimetic hydrogel scaffold gradually release CCL2 chemokine in situ preserving cytoarchitecture and promoting functional recovery in spinal cord injury. J Control Release. 2018;278:49–56. https://doi.org/10.1016/j.jconrel.2018.03.034.
23. Qu J, Zhang H. Roles of mesenchymal stem cells in spinal cord injury. Stem Cells Int. 2017;2017:5251313 https://doi.org/10.1155/2017/5251313.
24. Stewart AN, Matyas JJ, Welchko RM, Goldsmith AD, Zeiler SE, Hochgeschwender U, et al. SDF-1 overexpression by mesenchymal stem cells enhances GAP-43-positive axonal growth following spinal cord injury. Restor Neurol Neurosci. 2017;35:395–411. https://doi.org/10.3233/RNN-160678.
25. Yang EZ, Zhang GW, Xu JG, Chen S, Wang H, Cao LL, et al. Multichannel polymer scaffold seeded with activated Schwann cells and bone mesenchymal stem cells improves axonal regeneration and functional recovery after rat spinal cord injury. Acta Pharmacol Sin. 2017;38:623–37. https://doi.org/10.1038/aps.2017.11.
26. Tashiro K, Sephel GC, Weeks B, Sasaki M, Martin GR, Kleinman HK, et al. A synthetic peptide containing the IKVAV sequence from the A chain of laminin mediates cell attachment, migration, and neurite outgrowth. J Biol Chem. 1989;264:16174–82.
27. Tysseling-Mattiace VM, Sahni V, Niece KL, Birch D, Czeisler C, Fehlings MG, et al. Self-assembling nanofibers inhibit glial scar formation and promote axon elongation after spinal cord injury. J Neurosci. 2008;28:3814–23. https://doi.org/10.1523/JNEUROSCI.0143-08.2008.
28. Tysseling VM, Sahni V, Pashuck ET, Birch D, Hebert A, Czeisler C, et al. Self-assembling peptide amphiphile promotes plasticity of serotonergic fibers following spinal cord injury. J Neurosci Res. 2010;88:3161–70. https://doi.org/10.1002/jnr.22472.
29. Andrews MR, Czvitkovich S, Dassie E, Vogelaar CF, Faissner A, Blits B, et al. Alpha9 integrin promotes neurite outgrowth on tenascin-C and enhances sensory axon regeneration. J Neurosci. 2009;29:5546–57. https://doi.org/10.1523/JNEUROSCI.0759-09.2009.
30. Cheah M, Andrews MR, Chew DJ, Moloney EB, Verhaagen J, Fassler R, et al. Expression of an activated integrin promotes long-distance sensory axon regeneration in the spinal cord. J Neurosci. 2016;36:7283–97. https://doi.org/10.1523/JNEUROSCI.0901-16.2016.
31. Deumens R, Koopmans GC, Honig WM, Hamers FP, Maquet V, Jerome R, et al. Olfactory ensheathing cells, olfactory nerve fibroblasts and biomatrices to promote long-distance axon regrowth and functional recovery in the dorsally hemisected adult rat spinal cord. Exp Neurol. 2006;200:89–103. https://doi.org/10.1016/j.expneurol.2006.01.030.
32. Deumens R, Koopmans GC, Honig WM, Maquet V, Jerome R, Steinbusch HW, et al. Limitations in transplantation of astroglia-biomatrix bridges to stimulate corticospinal axon regrowth across large spinal lesion gaps. Neurosci Lett. 2006;400:208–12. https://doi.org/10.1016/j.neulet.2006.02.050.

33. Deng LX, Deng P, Ruan Y, Xu ZC, Liu NK, Wen X, et al. A novel growth-promoting pathway formed by GDNF-overexpressing Schwann cells promotes propriospinal axonal regeneration, synapse formation, and partial recovery of function after spinal cord injury. J Neurosci. 2013;33:5655–67. https://doi.org/10.1523/JNEUROSCI.2973-12.2013.
34. Iida T, Nakagawa M, Asano T, Fukushima C, Tachi K. Free vascularized lateral femoral cutaneous nerve graft with anterolateral thigh flap for reconstruction of facial nerve defects. J Reconstr Microsurg. 2006;22:343–8. https://doi.org/10.1055/s-2006-946711.
35. Glaser J, Gonzalez R, Sadr E, Keirstead HS. Neutralization of the chemokine CXCL10 reduces apoptosis and increases axon sprouting after spinal cord injury. J Neurosci Res. 2006;84:724–34. https://doi.org/10.1002/jnr.20982.
36. Gao XR, Xu HJ, Wang LF, Liu CB, Yu F. Mesenchymal stem cell transplantation carried in SVVYGLR modified self-assembling peptide promoted cardiac repair and angiogenesis after myocardial infarction. Biochem Biophys Res Commun. 2017;491:112–8. https://doi.org/10.1016/j.bbrc.2017.07.056.
37. Hou Y, Ryu CH, Jun JA, Kim SM, Jeong CH, Jeun SS. IL-8 enhances the angiogenic potential of human bone marrow mesenchymal stem cells by increasing vascular endothelial growth factor. Cell Biol Int. 2014;38:1050–9. https://doi.org/10.1002/cbin.10294.
38. Wang C, Poon S, Murali S, Koo CY, Bell TJ, Hinkley SF, et al. Engineering a vascular endothelial growth factor 165-binding heparan sulfate for vascular therapy. Biomaterials. 2014;35:6776–86. https://doi.org/10.1016/j.biomaterials.2014.04.084.
39. Golebiewska EM, Poole AW. Platelet secretion: from haemostasis to wound healing and beyond. Blood Rev. 2015;29:153–62. https://doi.org/10.1016/j.blre.2014.10.003.
40. Ullm S, Kruger A, Tondera C, Gebauer TP, Neffe AT, Lendlein A, et al. Biocompatibility and inflammatory response in vitro and in vivo to gelatin-based biomaterials with tailorable elastic properties. Biomaterials. 2014;35:9755–66. https://doi.org/10.1016/j.biomaterials.2014.08.023.
41. Feng Y, Li Q, Wu D, Niu Y, Yang C, Dong L, et al. A macrophage-activating, injectable hydrogel to sequester endogenous growth factors for in situ angiogenesis. Biomaterials. 2017;134:128–42. https://doi.org/10.1016/j.biomaterials.2017.04.042.